

AU8808958

ANSTO/E666

ANSTO/E666



**AUSTRALIAN NUCLEAR SCIENCE
AND TECHNOLOGY ORGANISATION
LUCAS HEIGHTS RESEARCH LABORATORIES**

MATHEMATICAL STUDY OF A LYSIMETER

by

D.K. GIBSON

NOVEMBER 1987

ISBN 0 642 59874 6

AUSTRALIAN NUCLEAR SCIENCE
AND TECHNOLOGY ORGANISATION
LUCAS HEIGHTS RESEARCH LABORATORIES

MATHEMATICAL STUDY OF A LYSIMETER

by

D.K. GIBSON

ABSTRACT

In studies of the rehabilitation of mine overburden heaps at Rum Jungle in the Northern Territory of Australia, simple buried water collectors have been used as lysimeters to measure the infiltration into the heaps. This report describes the development and results of a steady state finite difference computer code which calculates the movement of water in such systems. It is shown that the water collection efficiency of this type of lysimeter depends strongly on the hydraulic properties of the soil in which it is buried, as does the rate of capillary loss during periods of zero infiltration.

National Library of Australia card number and ISBN 0 642 59874 6

The following descriptors have been selected from the INIS Thesaurus to describe the subject content of this report for information retrieval purposes. For further details please refer to IAEA-INIS-12 (INIS: Manual for Indexing) and IAEA-INIS-13 (INIS: Thesaurus) published in Vienna by the International Atomic Energy Agency.

CLAYS; HYDRAULIC CONDUCTIVITY; LYSIMETERS; MATHEMATICAL MODELS; RUM JUNGLE; SOILS; WATER; WATER INFLUX;

EDITORIAL NOTE

From 27 April 1987, the Australian Atomic Energy Commission (AAEC) is replaced by Australian Nuclear Science and Technology Organisation (ANSTO). Serial numbers for reports with an issue date after April 1987 have the prefix ANSTO with no change of the symbol (E, M, S or C) or numbering sequence.

CONTENTS

1. INTRODUCTION	1	
2. COMPUTATION	1	
2.1 Description	1	
2.2 Basic equations	1	
2.3 Discretisation	2	
2.4 Boundary conditions	3	
2.5 Parameters	4	
2.6 Computer program	5	
3. RESULTS	5	
4. CONCLUSIONS	6	
5. ACKNOWLEDGEMENTS	6	
6. REFERENCES	6	
Figure 1	The calculated rate of infiltration into the lysimeter v. the surface infiltration rate for two different types of soil	7
Figure 2	Plot of the functions used to represent the hydraulic conductivities of the two soil types	7
Figure 3a	Ψ contours (m) for coarse sand and zero infiltration	8
Figure 3b	Ψ contours (m) for clay-loam and zero infiltration	8
Figure 3c	Ψ contours (m) for coarse sand with infiltration rate = $0.01 K_s$	9
Figure 3d	Ψ contours (m) for clay-loam with infiltration rate = $0.1 K_s$	9
Figure 3e	Ψ contours (m) for coarse sand with infiltration rate = $0.1 K_s$	10
Figure 3f	Ψ contours (m) for two-component model	10

1. INTRODUCTION

A simple type of lysimeter has been used to measure the infiltration of water through the clay layer used to seal White's Dump at the disused Rum Jungle uranium mine in the Northern Territory of Australia [Harries 1986]. The lysimeter consists of a metal drum, 900 mm deep and 600 mm diameter, filled with coarse gravel to a depth of 400 mm, and topped up with dump material. It was buried 300 mm below the clay layer which was placed on top of the dump as part of rehabilitation works. The dump is approximately 20 m high. The purpose of the gravel at the bottom of the lysimeter is to provide a region of high porosity to store the collected water and to provide at least a partial break in the capillary films which draw the water out of the lysimeter. The water level at the bottom of the drum has been monitored and maintained by a small access tube.

From the general principles of soil physics it can be seen that the increased moisture levels in the drum will cause water to be diverted from it, leading to a collection efficiency of less than 100 per cent [Hillel 1980]. The present mathematical analysis was instigated to provide quantitative information on the collection efficiency of the lysimeter, and also on the rate of water loss during extended periods of no infiltration. There are a number of general computer codes for solving flow in unsaturated media [e.g. UNSAT2, Neumann 1983]. However, for this problem the internal boundaries, representing the lysimeter base and walls, rendered these standard codes cumbersome to use. Therefore, there was a good case for writing a special purpose code, especially as two simplifications were appropriate. First, the cylindrical symmetry of the systems reduces the problem to two dimensions. Second, much insight can be gained from steady-state solutions; these solutions could also be quite relevant to the real situation as the infiltration from below the clay probably varies only slowly with time.

2. COMPUTATION

2.1 Description of Model

The system to be analysed is taken to be a small cylinder (the lysimeter) set centrally in a large one (the domain). The lower surface of the domain is saturated, representing the ground water table. A constant flux of water enters the top surface of the domain, representing the infiltration from the bottom of the clay layer. An objection could be raised against this assumption insofar that the moisture flow in the clay layer could be affected by the presence of the lysimeter. However, it has been shown in later calculations, in which provision was made for three different types of soil, that with the spacing used there was no significant perturbation of the water potentials in the clay layer by the saturated layer at the bottom of the lysimeter.

At first, the soil at the gravel layer boundary was taken to be saturated, implying the the gravel acted as a free draining gauze and that any water movement (*i.e.* drainage or capillary rise) was compensated by outflow or inflow at the lysimeter base. However, in reality the saturated layer at the bottom of the lysimeter is separated from the dump material by the low capillarity gravel. This work shows that it is necessary to incorporate the effect of the gravel layer more exactly by treating flow through the two regions of different hydraulic properties.

2.2 Basic Equations

The movement of water in a porous medium is described by the equation [Bear 1972]

$$\frac{\partial \theta(\psi)}{\partial t} = \nabla \cdot (K(\psi) \nabla \phi) \quad , \quad (1)$$

where θ = moisture content of the medium,
 $\psi(x,y,z,t)$ = the matric head of the medium,
 K = its hydraulic conductivity,
 ϕ = $\psi + z$ = the total head, and
 z = the height above a reference level.

Considering the time-independent case ($\partial \theta / \partial t = 0$) and converting to cylindrical co-ordinates, r, z with azimuthal symmetry, we have

$$\frac{1}{r} \frac{\partial}{\partial r} (rK \frac{\partial \phi}{\partial r}) + \frac{\partial}{\partial z} (K \frac{\partial \phi}{\partial z}) = 0. \quad (2)$$

Substituting $\psi+z$ for ϕ , we obtain

$$\frac{1}{r} \frac{\partial}{\partial r} (rK \frac{\partial \psi}{\partial r}) + \frac{\partial}{\partial z} (K \frac{\partial \psi}{\partial z}) + \frac{\partial K}{\partial z} = 0. \quad (3)$$

2.3 Discretisation

Numerical methods are necessary to obtain solutions of equation 3 for unrestricted functional forms of K. The finite difference method was used as it is the simplest to set up. The r, z plane is divided into a rectangular mesh with mesh sizes δr , δz . At each point the value of ψ , and hence the corresponding $K(\psi)$, is known. As a shorthand symbolism, the point under scrutiny is referred to as r_0, z_0 with corresponding ψ_0 and K_0 . The four nearest neighbouring points at $r-\delta r, r+\delta r, z-\delta z$ and $z+\delta z$ have values of $\psi_{-r}, K_{-r}, \psi_{+r}, \psi_{-z}$, etc.

At the intermesh point $r-\delta r/2$ we can write

$$rK \frac{\partial \psi}{\partial r} = (r_0 - \frac{\delta r}{2}) \frac{K_0 + K_{-r}}{2} \frac{\psi_0 - \psi_{-r}}{\delta r}.$$

Similarly at the other inter-mesh point, $r+\delta r/2$,

$$rK \frac{\partial \psi}{\partial r} = (r_0 + \frac{\delta r}{2}) \frac{K_0 + K_{+r}}{2} \frac{\psi_{+r} - \psi_0}{\delta r}.$$

Therefore, for the first term in equation 3 we may write

$$\frac{1}{r} \frac{\partial}{\partial r} (rK \frac{\partial \psi}{\partial r}) = \frac{1}{2r_0 \delta r^2} [(r_0 + \frac{\delta r}{2})(K_0 + K_{+r})(\psi_{+r} - \psi_0) - (r_0 - \frac{\delta r}{2})(K_0 + K_{-r})(\psi_0 - \psi_{-r})]. \quad (4)$$

Defining

$$R_+ = (r_0 + \frac{\delta r}{2})(K_0 + K_{+r}) / 2r_0 \delta r^2,$$

and

$$R_- = (r_0 - \frac{\delta r}{2})(K_0 + K_{-r}) / 2r_0 \delta r^2,$$

the right hand side of equation 4 becomes

$$R_+(\psi_{+r} - \psi_0) - R_-(\psi_0 - \psi_{-r}) - \psi_0(R_+ + R_-) = R_+\psi_{+r} + R_-\psi_{-r} - \psi_0(R_+ + R_-). \quad (5)$$

The second term in equation 3 can be treated similarly;

$$Z_+ = (K_{+z} + K_0) / 2\delta z^2,$$

$$\text{and } Z_- = (K_{-z} + K_0) / 2\delta z^2,$$

$$\frac{\partial}{\partial z} (K \frac{\partial \psi}{\partial z}) = Z_+\psi_{+z} + Z_-\psi_{-z} - \psi_0(Z_+ + Z_-).$$

For the third term of equation 3 we use the central difference formula

$$\frac{\partial K}{\partial z} = \frac{K_{+z} - K_{-z}}{2\delta z}.$$

Putting the three terms together we get for equation 3

$$\psi_0(R_+ + R_- + Z_+ + Z_-) - R_+\psi_{+r} - R_-\psi_{-r} - Z_+\psi_{+z} - Z_-\psi_{-z} - \frac{1}{2\delta z}(K_{+z} - K_{-z}) = F = 0. \quad (6)$$

Gauss-Seidel iteration was used to obtain the solution of equation 6 at all points. At each point a new value of ψ_0 , ψ_0' , was evaluated by

$$\psi_0' = \frac{R_+ \psi_{+r} + R_- \psi_{-r} + Z_+ \psi_{+z} + Z_- \psi_{-z} + \frac{1}{2\delta z} (K_{+z} - K_{-z})}{R_+ + R_- + Z_+ + Z_-}$$

This value, and its corresponding K_0' , immediately replaced K_0 and ψ_0 in their corresponding matrices.

The Gauss-Seidel-Newton method was also tried, where ψ_0' was calculated by

$$\psi_0' = \psi_0 - \frac{F}{\partial F / \partial \psi_0}$$

This method was not used because convergence was no faster than the the simpler method and computation time was longer.

2.4 Boundary Conditions

For simplicity, the lysimeter was assumed to have a thickness of one mesh length, thus separating the inner and outer boundaries. There are eight boundaries to be considered.

2.4.1 Central axis

The actual boundary condition is simply one of axial symmetry, expressed by $\partial\psi/\partial z = 0$. However, the discretisation of the first (r-dependent) term of equation 3, requires special treatment to avoid the singularity at $r = 0$. This term may be written

$$\frac{1}{r} \frac{\partial}{\partial r} (rK \frac{\partial\psi}{\partial r}) = \frac{1}{r} K \frac{\partial\psi}{\partial r} + \frac{\partial K}{\partial r} \frac{\partial\psi}{\partial r} + K \frac{\partial^2\psi}{\partial r^2}$$

L'Hopital's theorem gives

$$\lim_{r \rightarrow 0} \frac{1}{r} \frac{\partial\psi}{\partial r} = \frac{\partial^2\psi}{\partial r^2}$$

Also, from symmetry both $\frac{\partial K}{\partial r}$ and $\frac{\partial\psi}{\partial r}$ are zero at $r = 0$. Therefore

$$\begin{aligned} \frac{1}{r} \frac{\partial}{\partial r} (rK \frac{\partial\psi}{\partial r}) &= 2K \frac{\partial^2\psi}{\partial r^2} \quad \text{at } r = 0 \\ &= \frac{4K_0}{\delta r^2} (\psi_{+r} - \psi_0) \quad \text{in discrete form.} \end{aligned}$$

This can be expressed in the same form as equation 5

$$= R_+ \psi_{+r} + R_- \psi_{-r} - \psi_0 (R_+ + R_-)$$

provided that we define at $r = 0$

$$R_+ = R_- = \frac{2K_0}{\delta r^2},$$

and include the condition for radial symmetry $\psi_{+r} = \psi_{-r}$.

2.4.2 Cylindrical walls

On the side wall of the domain and on the inner and outer vertical walls of the lysimeter there is no radial flow.

Hence $\partial\psi/\partial r = 0$, which is achieved by putting $\psi_{+r} = \psi_{-r}$ for the concave boundaries and $\psi_{-r} = \psi_{+r}$ for the convex boundary.

2.4.3 Base of domain

This boundary represents the water table and always remains saturated. The condition is therefore $\psi = 0$ at $z = 0$.

2.4.4 Upper surface of domain

Infiltration is represented by a constant flux crossing the upper surface. The infiltration, q , taken as positive for a downward flux, is given by

$$q = K \frac{\partial\phi}{\partial z} ,$$
$$= K \frac{\partial}{\partial z} (\psi + z) ,$$

Therefore

$$\frac{\partial\psi}{\partial z} = \frac{q}{K} - 1.$$

This boundary condition is achieved by generating an artificial ψ_{+z} above the top surface according to

$$\psi_{+z} = \psi_{-z} + 2\delta z \left(\frac{q}{K_0} - 1 \right).$$

2.4.5 Base of lysimeter - internal

For the single soil model, the surface of the soil in contact with the gravel was assumed to be saturated, with $\psi = 0$. This surface acted as a source or sink of water, with the flux through it being the water collection (or loss) rate of the lysimeter.

When the hydraulic properties of the gravel layer were taken into account, this saturated layer was moved down to the lysimeter base. At the interface between the two soil types the hydraulic conductivity was taken to be the average of what would apply in the two adjoining regions.

2.4.6 Base of lysimeter - external

There is no axial flow from this surface, which makes it equivalent to the condition for the top surface of the domain with $q = 0$. The condition therefore is

$$\psi_{+z} = \psi_{-z} - 2\delta z.$$

2.5 Parameters

The parameters for the calculation fall into two groups; the geometrical size and shape of the domain and the lysimeter and the relationship $K(\psi)$. The domain was taken to be 6 m high, rather than the dump height of 20 m, as the extra height would entail using an inordinately large number of mesh points without adding to the understanding of the behaviour of the system. The geometrical parameters used for the computations are listed below:

Parameter	Value (m)
Diameter of the domain	3
Height of domain	6
Diameter of lysimeter	0.6
Height of lysimeter	0.9
Depth of gravel	0.4
Depth of top of lysimeter below top of domain	0.3

The hydraulic conductivity was defined by the formulae [Bear 1972]

$$K(\psi) = \frac{K_s}{1 + (\psi/\psi_e)^\alpha} \quad \text{for } \psi < 0 \quad (7a)$$

and $K(\psi) = K_s \quad \text{for } \psi \geq 0 \quad (7b)$

The three parameters needed to define the conductivity are the saturated conductivity, K_s , the air entry pressure, ψ_e and the exponent α . Values for these parameters were chosen for two markedly different soil types guided by the examples given by Talsma [1985], and are listed below:

Soil type	K_s (m day ⁻¹)	ψ_e (m)	α
Clay-loam	0.3	-0.3	2.4
Coarse sand	10	-0.08	5.7

2.6 Computer Program

The domain was represented by a matrix of ψ values, of the order of 100 by 100 points. Initial values of ψ were generated by assuming a uniform flux, q , throughout the domain, starting at $z = 0$. Convergence was checked by evaluating $\epsilon = \max |\psi_0 - \psi_0'|$. Convergence was slow; many hundreds of iterations were needed to give a stable result. The value of ϵ was not used as the criterion for sufficient iteration; a fixed number of iterations were performed and the final ψ matrix stored on a file. This was then available for examination, for example by plotting contours. The calculated flux balance was generally used as the proof of sufficient convergence. Agreement to within one to two per cent was achieved fairly readily with the grid sizes used. In some cases the stability of the ψ contours was a more sensitive test, especially for small infiltration rates, q .

The program was written in Fortran 77, in double precision. Typically about 10 to 15 minutes were needed for the calculation of each case on an IBM 4381 computer.

3. RESULTS

The results of the calculations for the single soil type model are summarised in figure 1, in which the water flux into the lysimeter is plotted against the input (infiltration) flux. The fluxes are expressed as fractions of the maximum flux, K_s . If the lysimeter is to provide an accurate measure of the infiltration rate, these two fluxes should be equal and the graph be a straight line at 45°. The computer model confirmed this for the 'sand' case, but for the 'clay' case large deviations from this result were found. For sand, the hydraulic conductivity drops very quickly as the matric potential, ψ , becomes increasingly negative (figure 2). This is because the capillary forces are weak in unsaturated sand. Hence the water movement is dominated by gravity, which drives it into the lysimeter, where it remains. For clay, on the other hand, the unsaturated hydraulic conductivity does not decrease nearly so fast, as the capillary forces are relatively much stronger. The difference in matric potential just above the lysimeter and next to it causes a sideways movement of soil moisture, thus reducing the flux to the lysimeter. Under these conditions the lysimeter is not a reliable device for measuring infiltration.

The fact that the lysimeter at Rum Jungle does collect water from small infiltration rates and loses water during the dry season at a slow rate indicates that the soil type (*i.e.* the dump material) resembles 'sand' in its hydraulic properties, which is to be expected of quarried rock. This accords with the calculations of capillary loss from the lysimeter with zero infiltration. With 'sand' the loss was essentially zero, but with 'clay' it came to about 1.2 mm/day. The loss measured at Rum Jungle during the dry season was about 0.03 mm/day, which is much lower than a clay soil would yield.

If the effect of the gravel is modelled more correctly, and the saturated surface taken to be at its base rather than at its top, the lysimeter records fluxes in clay soils somewhat more accurately than for the single soil type model. The 'gravel' was assumed to have the same properties as 'coarse sand' for these calculations. With an infiltration rate of 0.1 K_s the collection efficiency was 50 per cent for this case, compared with essentially zero efficiency with the simpler model. Contour plots of the ψ potentials are shown for various cases in figure 3.

4. CONCLUSIONS

The behaviour of a simple catchment lysimeter has been shown to be very dependent on the nature of the soil in which it operates. For low capillarity soils (sand or gravel) the lysimeter records the infiltration rate correctly. In the case of high capillarity soils (clay or loam), this type of lysimeter should be treated cautiously as it will record very low infiltration rates unless proper precautions are taken. Sufficient attention to the grading of the soil in the lysimeter could suffice to obtain accurate records. Alternatively, if the lysimeter could be positioned either at the surface or so that its base coincided with the ground water table, the problems revealed by this analysis would be avoided.

5. ACKNOWLEDGEMENTS

It is a pleasure to acknowledge the support of Dr A I M Ritchie, Dr J R Harries and Dr G Pantelis, and especially the assistance of the latter with the mathematical formulation.

6. REFERENCES

- Bear, J. [1972] - *Dynamics of Fluids in Porous Media*. Elsevier, New York.
- Harries, J. R. [1986] - Private communication.
- Hillel, D. [1980] - *Fundamentals of Soil Physics* Academic Press, New York.
- Neumann, S. [1983] - Documentation and User's Guide: UNSAT2 - Variably Saturated Flow Model. NUREG/CR - 3390 : WWL/TM - 1791 - 1
- Talsma, T [1985] Prediction of hydraulic conductivity data from soil water retention data. *Soil Sci.*, 140: 184-188

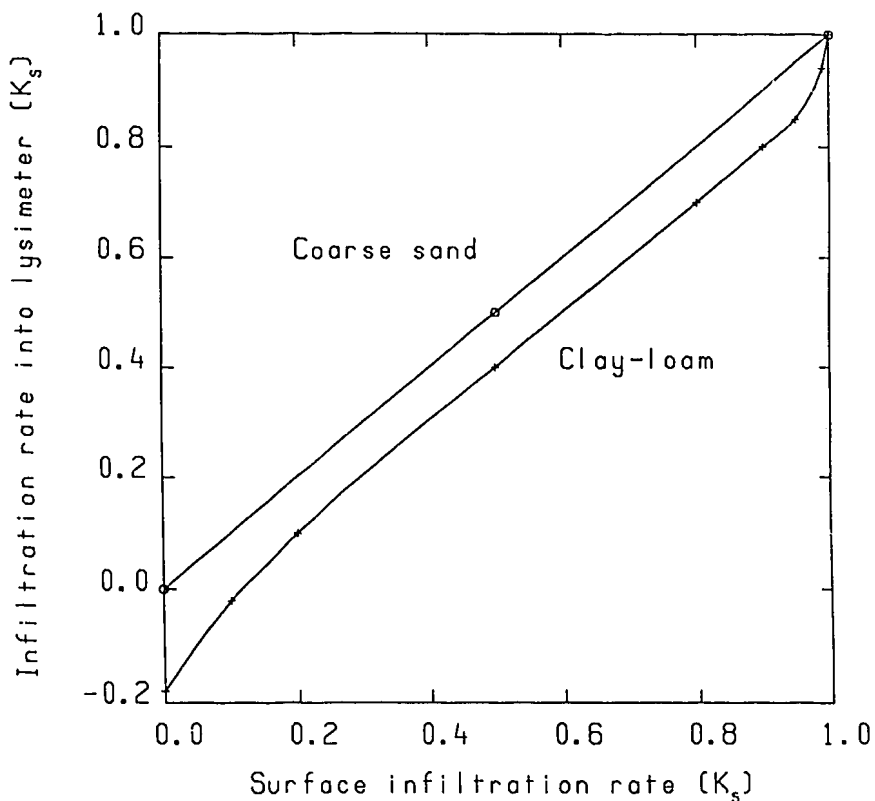


Figure 1 The calculated rate of infiltration into the lysimeter v. the surface infiltration rate for two different types of soil. The rates are expressed as fractions of the saturated hydraulic conductivity of the soil in question.

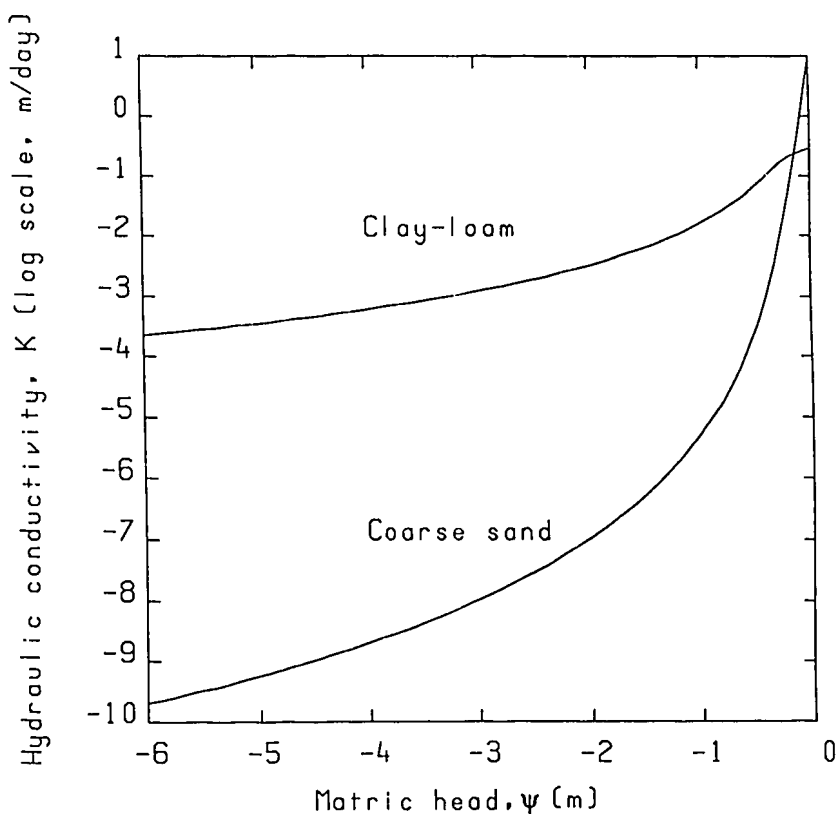


Figure 2 Plot of the functions used to represent the hydraulic conductivities of the two soil types.

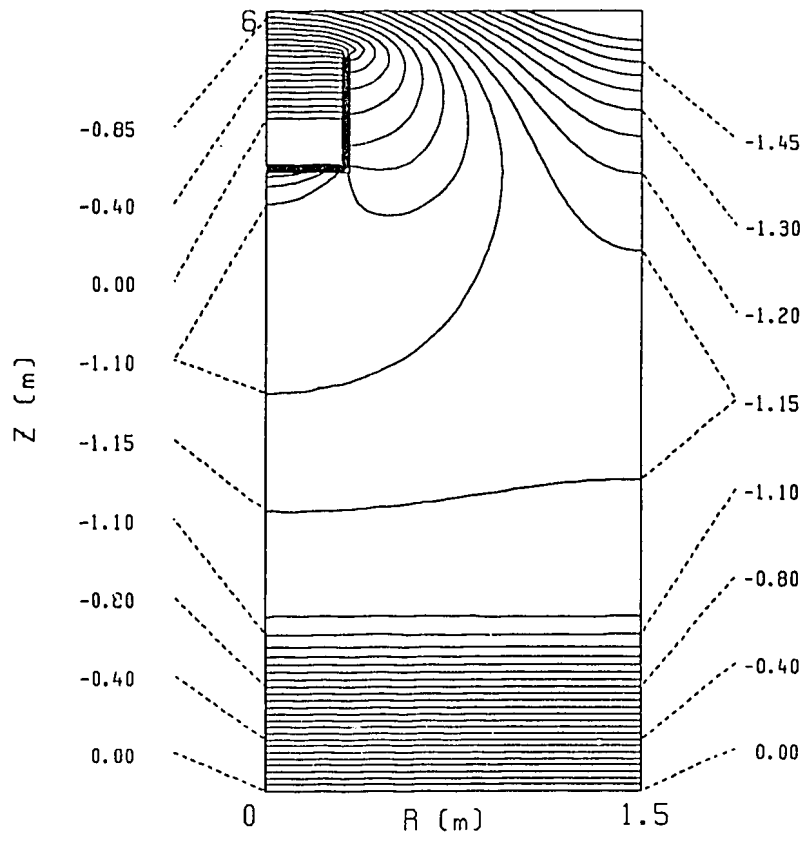


Figure 3a ψ contours (m) for coarse sand and zero infiltration.

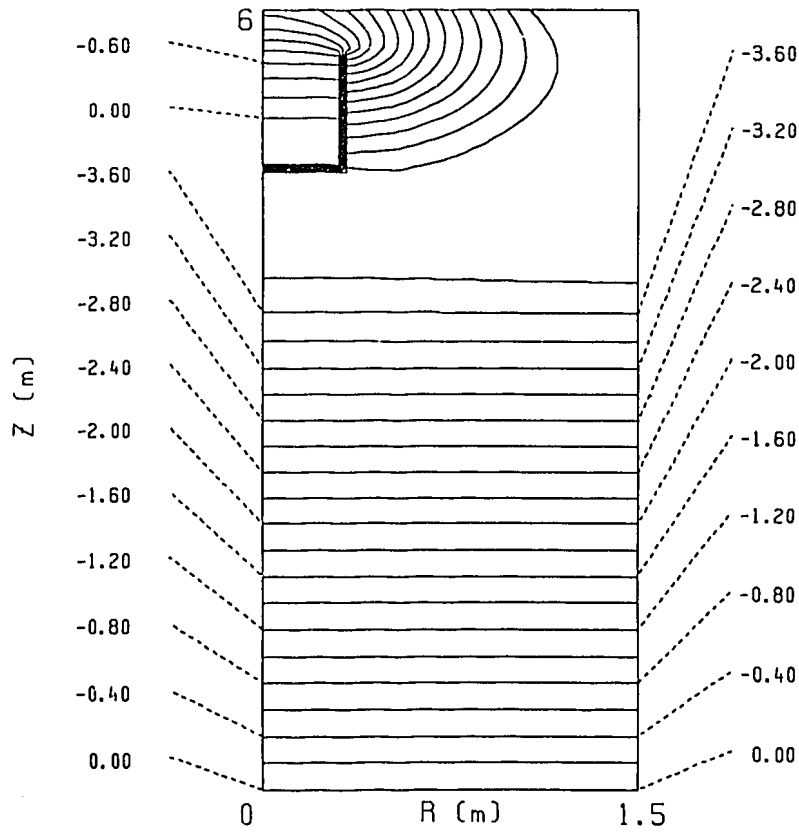


Figure 3b ψ contours (m) for clay-loam and zero infiltration.

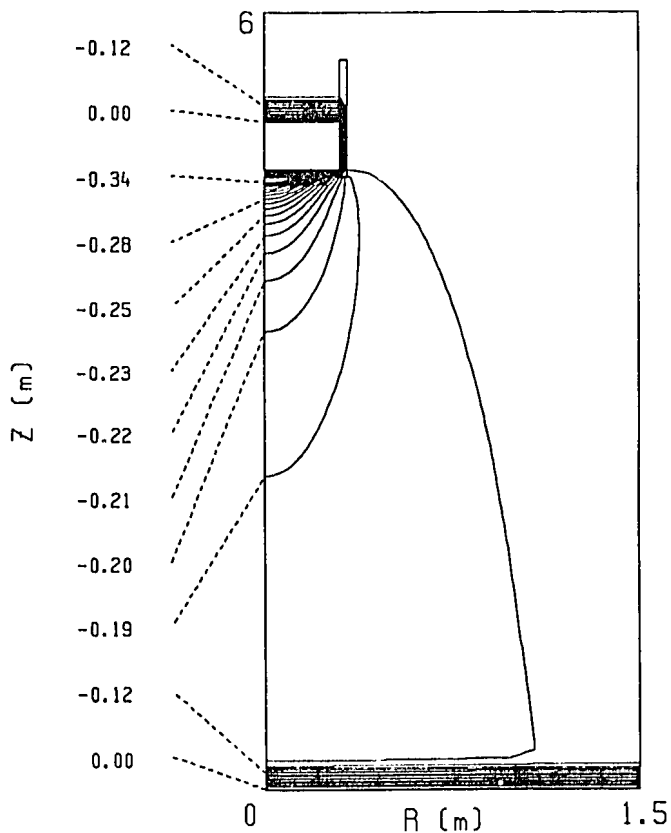


Figure 3c ψ contours (m) for coarse sand with infiltration rate = $0.01 K_s$.

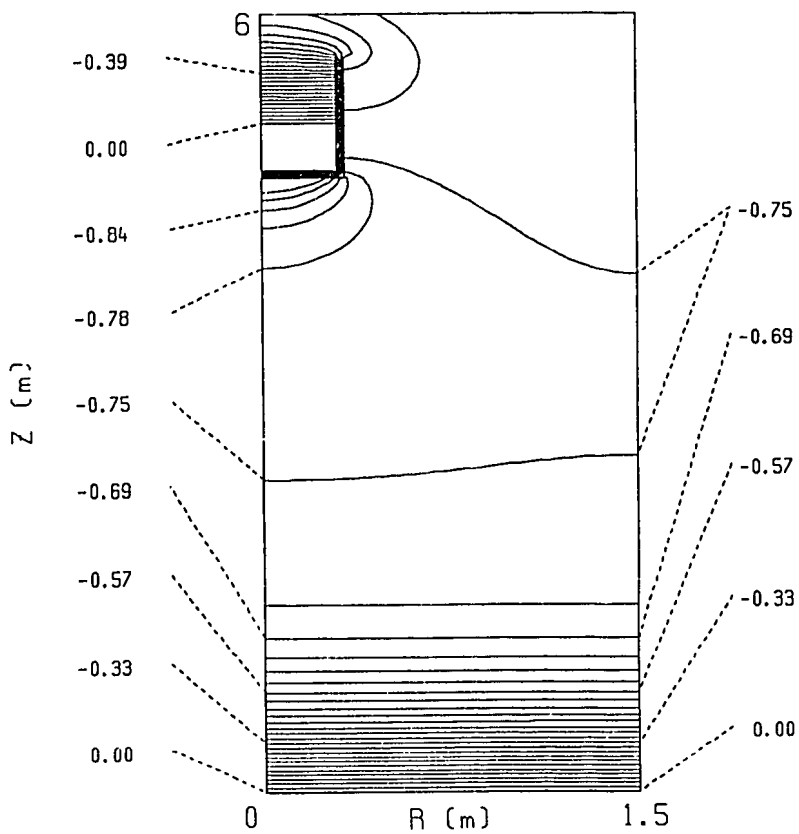


Figure 3d ψ contours (m) for clay-loam with infiltration rate = $0.1 K_s$.

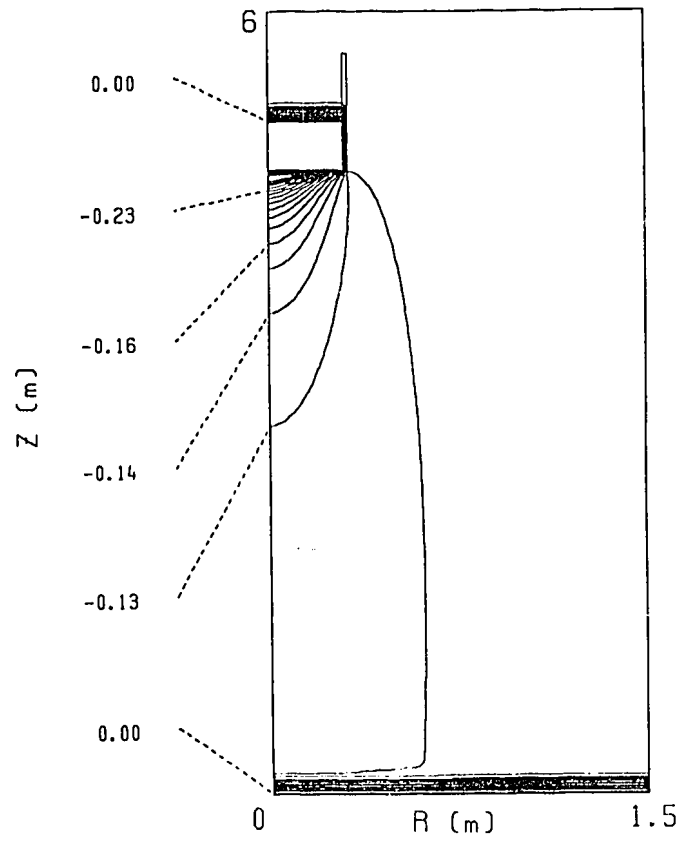


Figure 3e ψ contours (m) for coarse sand with infiltration rate = $0.1 K_s$.

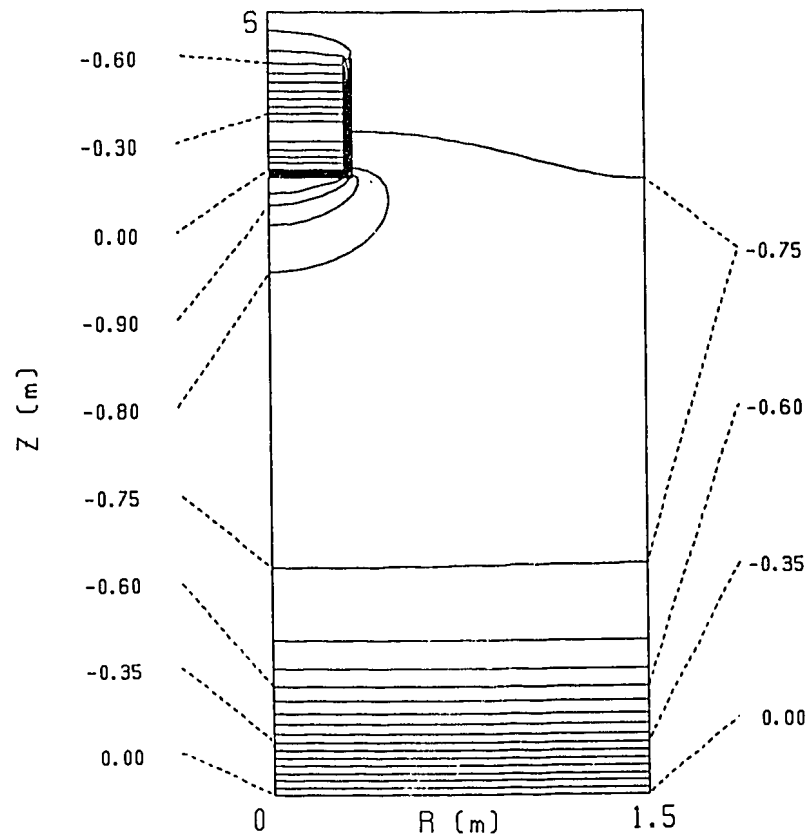


Figure 3f ψ contours (m) for two-component model. The main soil type is clay-loam and the porous gravel is represented by the coarse sand hydraulic function.